IWLHS, 20-22/02/2013, Aachen - Bung & Pagliara (eds) - © 2013 Bundesanstalt für Wasserbau ISBN 978-3-939230-04-5

Flat and Pooled Stepped Spillways for Overflow Weirs and Embankments: Cavity Flow Processes, Flow Aeration and Energy Dissipation

P. Guenther, S. Felder & H. Chanson
The University of Queensland, School of Civil Engineering, Brisbane QLD 4072, Australia

ABSTRACT: For overflow weirs and embankments, the stepped chute profile may increase the rate of energy dissipation on the waterway. Herein four different stepped chute configurations were tested with a focus on the cavity flow processes, flow aeration and energy dissipation performances. Detailed flow visualisations and air-water flow measurements were conducted for all configurations. The results highlighted the strong flow aeration. The residual energy was the lowest for the flat stepped weir. The data for the stepped spillway configuration with in-line and staggered configurations of flat and pooled steps showed large differences in terms of residual head in the transverse direction consistent with the three-dimensional flow motion. The in-line and staggered configurations did not provide any advantageous performances in terms of energy dissipation and flow aeration, and they were affected by three-dimensional patterns leading to some flow concentration.

Keywords: Stepped spillways, Weirs, Embankments, Flat steps, Pooled steps, Cavity ejection, Energy dissipation, Flow aeration, Residual head

1 INTRODUCTION

Worldwide the design floods of several reservoirs were re-evaluated and the revised spillway outflow was typically larger than that used in the original design. The occurrence of these larger floods could result in dam overtopping with catastrophic consequences when an insufficient storage or spillway capacity is available. A number of overtopping protection systems were developed for embankments and earthfill dams. These include concrete overtopping protection systems, timber cribs, sheet-piles, riprap and gabions, reinforced earth, minimum energy loss (MEL) weirs, embankment overflow stepped spillways and the precast concrete block protection systems developed by the Russian engineers (ASCE 1994, Chanson 2009a). During the last three decades, a number of embankment dam stepped spillways were built with a range of construction techniques, including gabions, reinforced earth, pre-cast concrete slabs and roller compacted concrete (RCC) (Chanson 1995,2001). The stepped profile is designed to increase the rate of energy dissipation on the chute (Chanson 2001, Ohtsu et al. 2004) and the design engineers must assess accurately the turbulent kinetic energy dissipation above the steps, in particular for large discharges per unit width corresponding to the skimming flow regime. A characteristic feature of skimming flows is the high level of turbulence and free-surface aeration (Rajaratnam 1990, Peyras et al. 1992). The water flows downs the steps as a coherent free-stream skimming over the pseudo-bottom formed by the step edges. In the step cavities, the turbulent recirculation is maintained through the transmission of shear stress from the free-stream. At the free-surface, air is continuously trapped and released, and the resulting two-phase mixture interacts with the flow turbulence yielding some intricate air-water structure associated with complicated energy dissipation mechanisms (Chanson & Toombes 2002, Gonzalez & Chanson 2008).

Although the prediction of the turbulent dissipation constitutes a critical design stage, the present literature is skewed towards steep slopes with flat horizontal steps, typical of modern gravity dams. In the present study, new measurements were conducted in a large facility with a channel slope of 26.6º (2H:1V) and step heights of 0.10 m. Four stepped geometries were tested: flat horizontal steps, pooled

steps, and in-line and staggered configurations of flat and pooled steps. The focus of the present works was on the cavity ejection processes, flow aeration and energy dissipation performances.

2 PHYSICAL MODELLING AND INSTRUMENTATION

2.1 *Presentation*

In free-surface flows, a dimensional analysis gives a series of dimensionless relationships between the two-phase flow properties at a dimensionless location along the chute and the channel characteristics, inflow properties and fluid properties (Chanson & Gonzalez 2005, Felder & Chanson 2009). When the same fluids, air and water, are used in models and prototype, the independent parameters include both Froude and Reynolds numbers, since the Morton number is an invariant (Wood 1991, Chanson 2009b, Pfister & Chanson 2012).

Traditionally, the experiments are conducted based upon an undistorted Froude similitude, but it is nearly impossible to achieve a true dynamic similarity of high-velocity air–water flows in small size laboratory models because of the number of relevant dimensionless parameters. Recent results demonstrated that the physical studies must be conducted in large size facilities operating at large Reynolds numbers to minimise viscous scale effects (Felder & Chanson 2009). Herein the study was performed based upon an undistorted Froude similarity and the experimental flow conditions were selected to achieve large dimensionless discharges corresponding to Reynolds numbers ranging from 1×10^4 to 1×10^6.

2.2 *Experimental flume and instrumentation*

New experiments were performed at the University of Queensland on a large stepped spillway model with a slope of 26.6º (2H:1V). The experimental facility was newly designed. It consisted of a broad-crested weir with upstream rounded corner followed by a 0.52 m wide (W = 0.52 m) stepped chute made of 10 steps (h = 0.10 m, l = 0.2 m). Constant flow rates were supplied by a large upstream intake basin with a size of 2.9 m × 2.2 m and a depth of 1.5 m, and smooth inflows to the test section were delivered through a 4.23:1 smooth convergent.

The air-water flow measurements were conducted with a two-tip phase detection intrusive probe (Ø = 0.25 mm, Δx = 7.2 mm, Δz = 1.5 mm). The probe was excited by an air-bubble detector (Ref. UQ82.518) and sampled at 20 kHz per tip for 45 s. The measurements were performed at all step edges downstream of the inception point of free surface aeration. Herewith the raw data yielded the void fraction C, bubble count rate F, and interfacial velocity V. Further observations were conducted with a HD video camera Sony™ HDR-XR160E (Standard HQ HD quality 25 fps), two dSLR camera Pentax™ K-7 and Canon™ 450D. More details on the experimental facility, instrumentation and experimental data were reported in Felder et al. (2012).

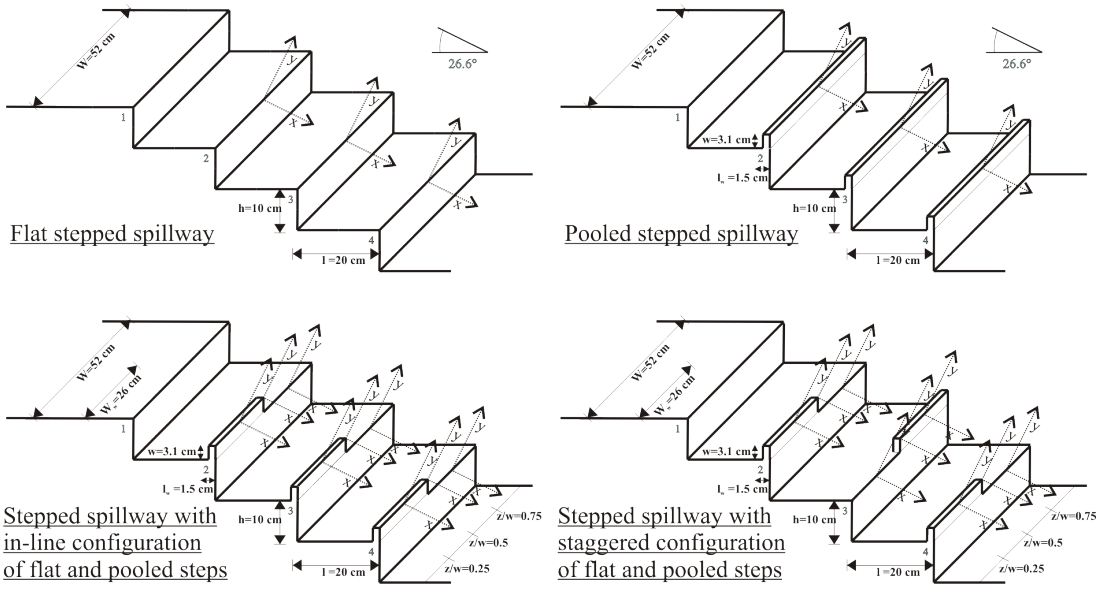

Figure 1. Definition sketch of the stepped configurations

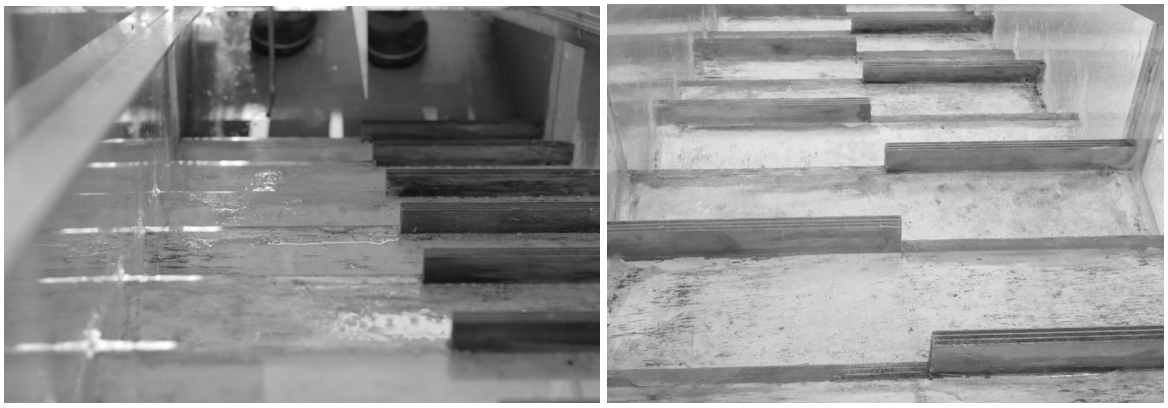

Figure 2. Photographs of the stepped configurations with in-line (Left) and staggered (Right) stepped arrangements - View from upstream looking downstream

2.3 *Experimental investigations*

The experimental study was conducted for four stepped spillway configurations (Fig. 1 & 2). These were a stepped spillway with flat horizontal steps, a pooled stepped spillway with weir height w = 0.031 m, and two stepped spillways with in-line and staggered configurations of flat and pooled steps. The in-line stepped spillway configuration consisted of pooled steps (w = 0.031 m) and flat steps in-line for half the channel width (W_w = W/2 = 0.26 m). The staggered pooled stepped spillway configuration was characterised by alternating flat and pooled steps. On the flat and pooled stepped spillways, the air-water flow measurements were conducted on the channel centreline. For the in-line and staggered configurations, the measurements were performed at three transverse locations: z/W = 0.25, 0.5 (centreline) & 0.75.

The flow patterns were observed for a wide range of discharges $0.002 \leq Q \leq 0.155$ m^3/s. The air-water flow measurements were performed for discharges within $0.013 \leq Q \leq 0.130$ m^3/s corresponding to Reynolds numbers between 1×10^5 to 1×10^6. Most two-phase flow experiments were conducted in the transition and skimming flow regimes.

3 FLOW PATTERNS

The visual investigations of the flow patterns included the observations of the air-water flow patterns for all stepped spillway configurations for a broad range of discharges. For some low discharges, the air-water flows on the pooled stepped spillway exhibited some small instabilities linked with some pulsations for small discharges. The flow processes on the stepped spillways with in-line and staggered configurations of flat and pooled steps showed some three-dimensional air-water flow features including standing sidewall waves and supercritical shockwaves.

The flat stepped spillway showed some typical flow patterns with nappe ($d_c/h < 0.5$), transition ($0.5 < d_c/h < 0.9$) and skimming flow ($d_c/h > 0.9$) regimes depending upon the dimensionless flow rate d_c/h, where d_c is the critical flow depth. Some similar flow regimes were observed on the pooled stepped spillway (Fig. 3), although some pulsating flow was seen for some nappe flow rate. For the smallest flow rates ($d_c/h < 0.45$), a nappe flow regime was observed on the pooled stepped chute and the water discharged in a succession of free falling nappes from one step pool to the following. However, for $0.3 \leq d_c/h \leq 0.45$, a pulsating flow was observed in the first step cavity leading to some small instability of the following free-falling nappes. The pulsations in the first step cavity were periodic and had a frequency of about 1 Hz (1 s period) for $d_c/h = 0.3$. These pulsations were seen about every 5 seconds for $d_c/h = 0.45$. The pulsating mechanism was comparable to the self-induced instabilities on pooled stepped spillways with slopes $\theta = 8.9°$ & 30º (Thorwarth 2008, Felder & Chanson 2012, Takahashi et al. 2008). For intermediate flow rates $0.45 \leq d_c/h \leq 0.97$, a transition flow regime was observed with some strong splashing in the air-water flow region downstream of the inception point of air-entrainment. For larger discharges $d_c/h > 0.97$, a skimming flow regime occurred with some stable recirculation motions in the step cavities (Fig. 3, Right). At the upstream end of the chute, the flow was transparent (clear-waters) and the water surface was parallel to the pseudo-bottom formed by the pool step weirs equivalent to skimming flows on flat stepped spillways. The flow depth however was larger than on flat stepped chutes because of the pool height. Downstream of the inception point of free-surface aeration, the flow was highly aerated.

Figure 3. Skimming flow regime on flat and pooled stepped spillways - Left: flat steps, Q = 0.114 m^3/s, d_c/h = 1.7, Re = 8.8×10^5; Right: pooled steps, Q = 0.100 m^3/s, d_c/h = 1.56, Re = 7.7×10^5

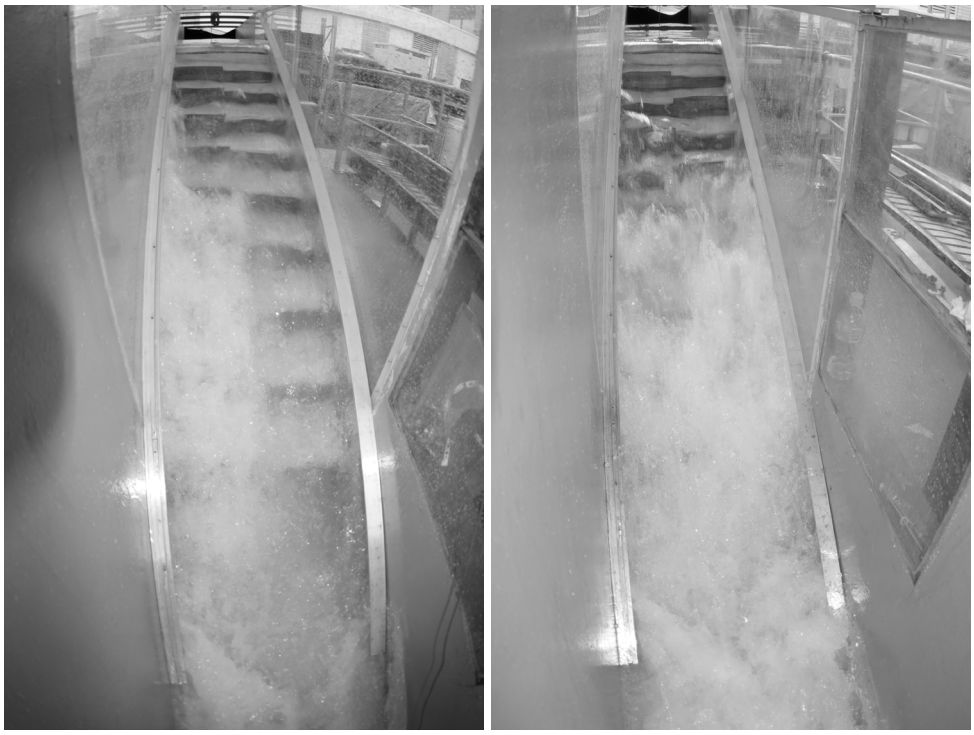

Figure 4. Three-dimensionless flow down the in-line and staggered configurations of flat and pooled steps - Left: in-line configuration, Q = 0.098 m^3/s, d_c/h = 1.54, Re = 7.6×10^5; Right: staggered configuration, Q = 0.090 m^3/s, d_c/h = 1.45, Re = 6.9×10^5

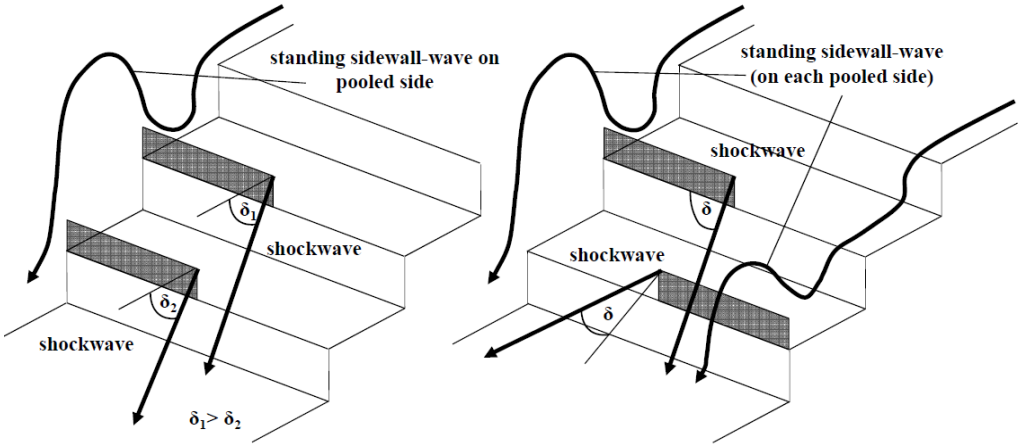

Figure 5. Sketches of sidewall standing waves and shock waves in stepped chutes with inline (Left) and staggered (Right) configurations of flat and pooled steps

On the in-line and staggered configurations of flat and pooled steps, the flow was highly three-dimensional (Fig. 4). Standing sidewall waves and shockwaves were observed along the sidewalls and on channel centreline respectively (Fig. 5), and these instabilities were associated with some strong splashing. On the in-line configuration, the pool weirs induced larger air-water depths at the pooled side of the

channel, and a faster flow motion was observed at the flat stepped side (Fig. 4, Left). The formation of nappe, transition and skimming flows could be determined separately on both sides. For small flow rates ($d_c/h < 0.46$), a nappe flow regime was observed on both sides of the spillway chute with plunging jets from step to step on the flat side and from pool to pool on the pooled side. Some transverse flow motions as well as strong droplet ejections were seen along the entire channel length. With increasing discharges ($0.46 < d_c/h < 0.57$), the flow became more unstable: it was characterised by plunging jets interacting on channel centreline together with a chaotic flow behaviour. The pools induced large flow disturbances and some three-dimensional flow motion was observed. For $0.57 < d_c/h < 0.86$, a transition flow regime was observed on both sides of the channel with some distinct droplet ejection downstream of the inception point of aeration. Some transverse flow interactions took place on channel centreline and yielded some three-dimensional flow motions along the entire channel. An intermediate flow regime ($0.86 < d_c/h < 1.03$) was characterised by a skimming flow regime on the pooled stepped side, and some transition flow on the flat stepped side of the spillway. Generally, the three-dimensional flow motion and flow disturbances caused by the pools became less significant with increasing discharges. For $d_c/h > 1.03$, a skimming flow was observed on both sides of the channel. The skimming flows showed some similarities to those observed on the flat stepped and pooled stepped spillways (Fig. 4, Left). The flow showed comparatively larger droplet ejections and the recirculation processes in the cavities appeared more irregular and disturbed compared to the uniform flat and pooled stepped spillways.

On the staggered stepped configuration, a nappe flow regime was observed at low flow rates ($d_c/h < 0.56$). A wavy flow appearance from side to side was observed along the entire channel length. The jets were highly aerated and showed some distinct plunge heights. For $0.56 < d_c/h < 0.92$, a transition flow occurred along the stepped chute. Some jets plunged over each second adjacent step edge. The step cavities of both flat and pooled steps showed no air pockets. The air-water mixture was highly aerated, showing some pseudo-chaotic pattern and transverse interactions on the channel centreline. The waving appearance of the flow from side to side became less significant than in the nappe flow regime. For $d_c/h > 0.92$, a skimming flow regime was observed (Fig. 4, Right). The recirculation in the step cavities was observed, although the recirculation processes were unsteady and disturbed by the staggered step configuration. The flow appeared highly aerated.

The stepped spillways with in-line and staggered configuration of flat and pooled steps showed some irregular occurrence of standing sidewalls and shockwaves for all flow regimes. The sidewall standing wave lengths and heights were comparable for both in-line and staggered configurations of flat and pooled steps. With increasing discharges, both wave height and length became smaller. The shockwaves occurred predominantly on the spillway centreline and the direction of the shockwaves differed between adjacent steps depending upon the configuration (Fig. 5). Further informations on the flow instabilities were reported by Felder et al. (2012).

4 CAVITY FLOW PROCESSES

On the flat and pooled stepped spillways, the cavity ejections were carefully observed. The recirculation processes were documented for each step cavity at and downstream of the inception point of free surface aeration. The clear-water surface upstream of the inception point appeared two-dimensional and parallel to the pseudo-bottom formed by the step edges and pooled weir edges respectively. Close to the inception point, the surface showed an irregular flapping mechanism which led to some waving behaviour. The surface tended to lean inward the cavity at irregular intervals and caused an air packet entrapment which was advected in the form of smaller and uniform shaped bubbles within the step cavities (Fig. 6, Left). This pattern was consistent with previous observations on stepped spillways (Chamani 2000, Chanson 2001, Toombes & Chanson 2007). With increasing discharge, the flapping mechanism of the free-surface became less distinct. Visually the flow resistance caused by the next downstream step, or pool edge, yielded some ejection processes close to the respective step or pool edge. Figure 6 illustrates the flapping mechanism and the cavity ejection processes on the flat and pooled stepped spillways. The cavity ejection processes were similar in appearance for the flat and pooled steps.

Basically the cavity recirculation observations highlighted some distinct ejection processes with inward and outward cavity flow motion. These occurred at irregular time intervals and led to some additional air entrainment. The ejections appeared to be sequential from upstream to downstream as illustrated by Djenidi et al. (1999) and Chanson et al. (2002). On average, the data indicated a slight increase in cavity ejection rate with increasing downstream distance for a given flow rate (Fig. 7, Left). The results are summarised in Figure 7 (Right) showing the median cavity ejection frequency as a function of the Rey-

nolds number. Indeed the ejection processes took place in regions of high shear stress where the Reynolds number was closely linked to turbulence properties.

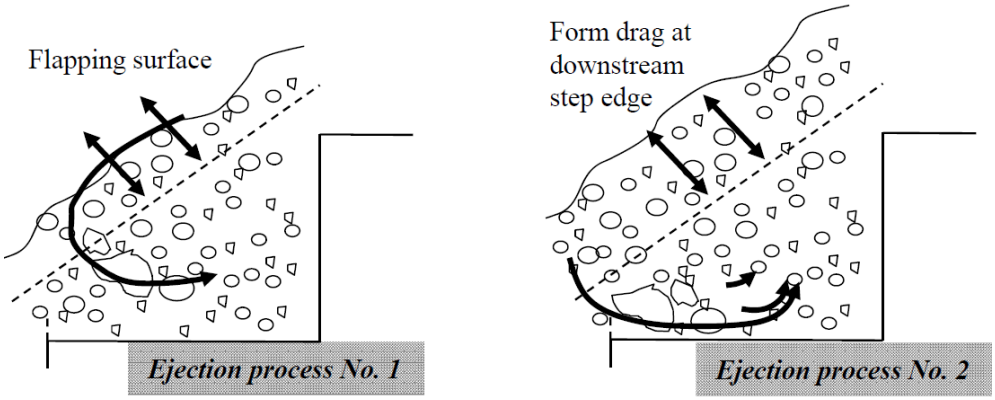

Figure 6. Sketch of cavity ejection processes on flat and pooled stepped spillways (θ = 26.6°)

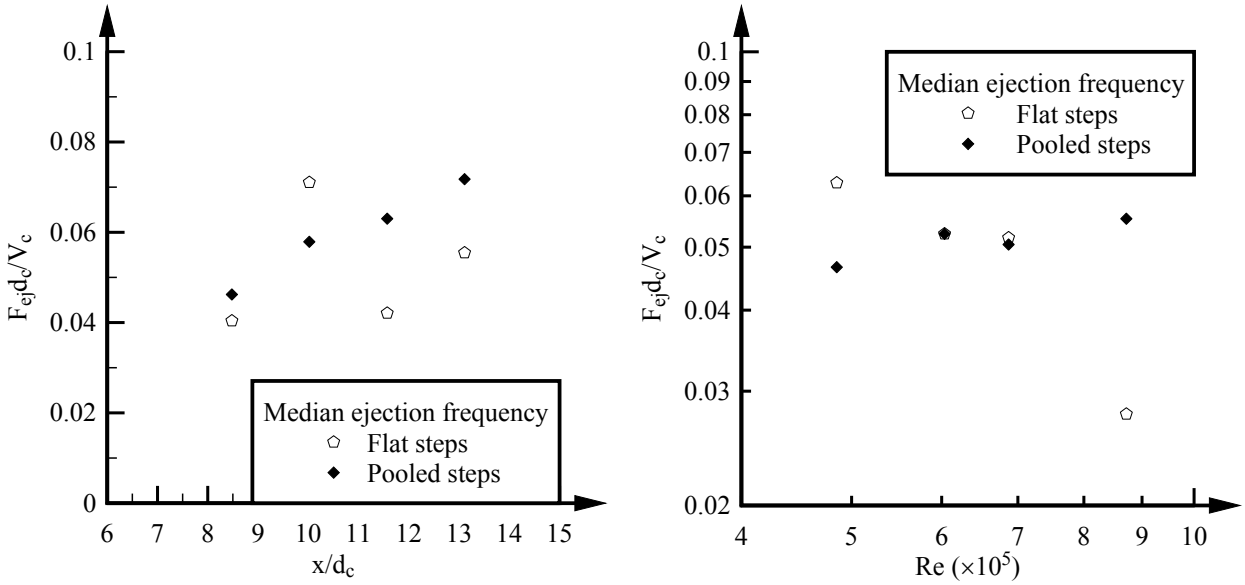

Figure 7. Dimensionless cavity ejection frequency $F_{ej}d_c/V_c$ on flat and pooled stepped spillways (θ = 26.6°) - Left: Longitudinal distribution in skimming flow (d_c/h = 1.45, Re=6.9×10^5); Right: median ejection frequency as a function of Reynolds number

The cavity ejection process in a skimming flow on stepped spillway may be analysed in term of energy considerations, assuming that all the energy losses took place by viscous dissipation in the cavity, with some energy exchange between the main stream and the recirculation by irregular fluid ejection. The results yielded an expression of the averaged ejection frequency F_{ej} as a function of the Darcy-Weisbach friction factor f_e:

$$\frac{F_{ej} \times (h \times \cos\theta)}{U_w} \approx \frac{f_e}{2 \times \lambda \times \eta} \qquad (1)$$

where U_w = flow velocity, h = vertical step height, θ = angle between the pseudo-bottom formed by the step edges and the horizontal, λ = ratio of average fluid ejection volume to total cavity volume, and η = ratio of average ejection period to burst duration. Equation (1) was developed for a wide chute with flat horizontal steps assuming a gradually-varied flow motion close to uniform equilibrium. The reasoning may be extended to a pooled stepped chute:

$$\frac{F_{ej} \times (h \times \cos\theta)}{U_w} \approx \frac{f_e}{2 \times \lambda \times \eta \times \left(1 + 2 \times \frac{w}{h}\right)} \qquad (2)$$

where w = vertical pool height. Equation (2) is valid for a wide chute with horizontal steps and vertical pool walls.

Herein the average ejection period to burst duration was on average $\eta \approx 3.5$. While the video analyses did not provide accurate information about the average fluid ejection volume ratio, the combination of flow resistance data and the above equations (1) and (2) would yield meaningless values of λ (i.e. $\lambda > 1$). The result might suggest the over-simplification of Equations (1) and (2) to assume that "all the energy losses took place by viscous dissipation in the cavity".

5 AIR-WATER FLOW PROPERTIES

Detailed air-water flow measurements were performed for all four configurations. Overall the results highlighted the intense flow aeration. Downstream of the inception of free-surface aeration, the entire water column including the step cavities were aerated (Fig. 8). Figure 8 shows some dimensionless distributions of void fraction for all four stepped configurations. In Figure 8, y is the distance normal to the pseudo-bottom formed by the step edges with y = 0 at the step edges for flat steps and y = 0 at the weir edge for the pooled steps. The skimming flow data compared favourably with an analytical solution of the air bubble diffusion equation:

$$C = 1 - \tanh^2\left(K' - \frac{y/Y_{90}}{2 \times D_o} + \frac{(y/Y_{90} - 1/3)^3}{3 \times D_o}\right) \qquad (3)$$

where Y_{90} = characteristic distance where C = 0.90, and K', D_o = dimensionless functions of the depth-averaged void fraction C_{mean} (Chanson and Toombes 2002). Equation (3) is compared with experimental data in Figure 8.

Overall the void fraction data showed close results between flat and pooled steps within the main stream (Fig. 8, Top left). In skimming flows, the depth-averaged void fraction ranged between 0.3 and 0.35 for both geometries. On the in-line configuration of flat and pooled steps, the measurements showed some transverse differences (Fig. 8, Top right). The flow was significantly more aerated on the pooled side (z/W = 0.25) as illustrated by the photographs (Fig. 4 Left). On the staggered configuration of flat and pooled steps, the void fraction distributions were more uniformly distributed across the channel width, although the alternation of flat and pooled steps every second step edge induced locally some three-dimensional flow motion.

The interfacial velocity distributions (data not shown) exhibited a self-similar profile on both flat and pooled stepped spillways:

$$\frac{V}{V_{90}} = \left(\frac{y}{Y_{90}}\right)^{1/N} \qquad y/Y_{90} < 1 \text{ (4a)}$$

$$\frac{V}{V_{90}} = 1 \qquad y/Y_{90} > 1 \text{ (4b)}$$

with V_{90} = characteristic velocity at $y = Y_{90}$. The exact value of N varied slightly from one step to the next step for a given flow rate with a typical value N = 10, while Kökpinar (2004) observed N = 6 on flat and pooled stepped chutes ($\theta = 30°$).

On the in-line and staggered configurations of flat and pooled steps, the velocity distributions followed closely Equation (4a) for $y/Y_{90} < 1$ at all transverse locations, but velocity data in the spray region incl. $y/Y_{90} > 1$ were scattered. On the in-line configuration, the interfacial velocities were consistently larger on the flat stepped side than on the pooled stepped side of the chute. Some transverse flow motion was observed along the channel centreline with the staggered configuration of flat and pooled steps, leading to an alternation of transverse flow direction between each step.

6 ENERGY DISSIPATION

The rate of energy dissipation above the stepped chute and the residual energy at the downstream end of the stepped spillway are two key design parameters, especially for low-head weirs. In this study, the rate of energy dissipation and the residual energy were estimated for all stepped spillway configurations based upon the detailed air-water flow measurements. The residual head was estimated as:

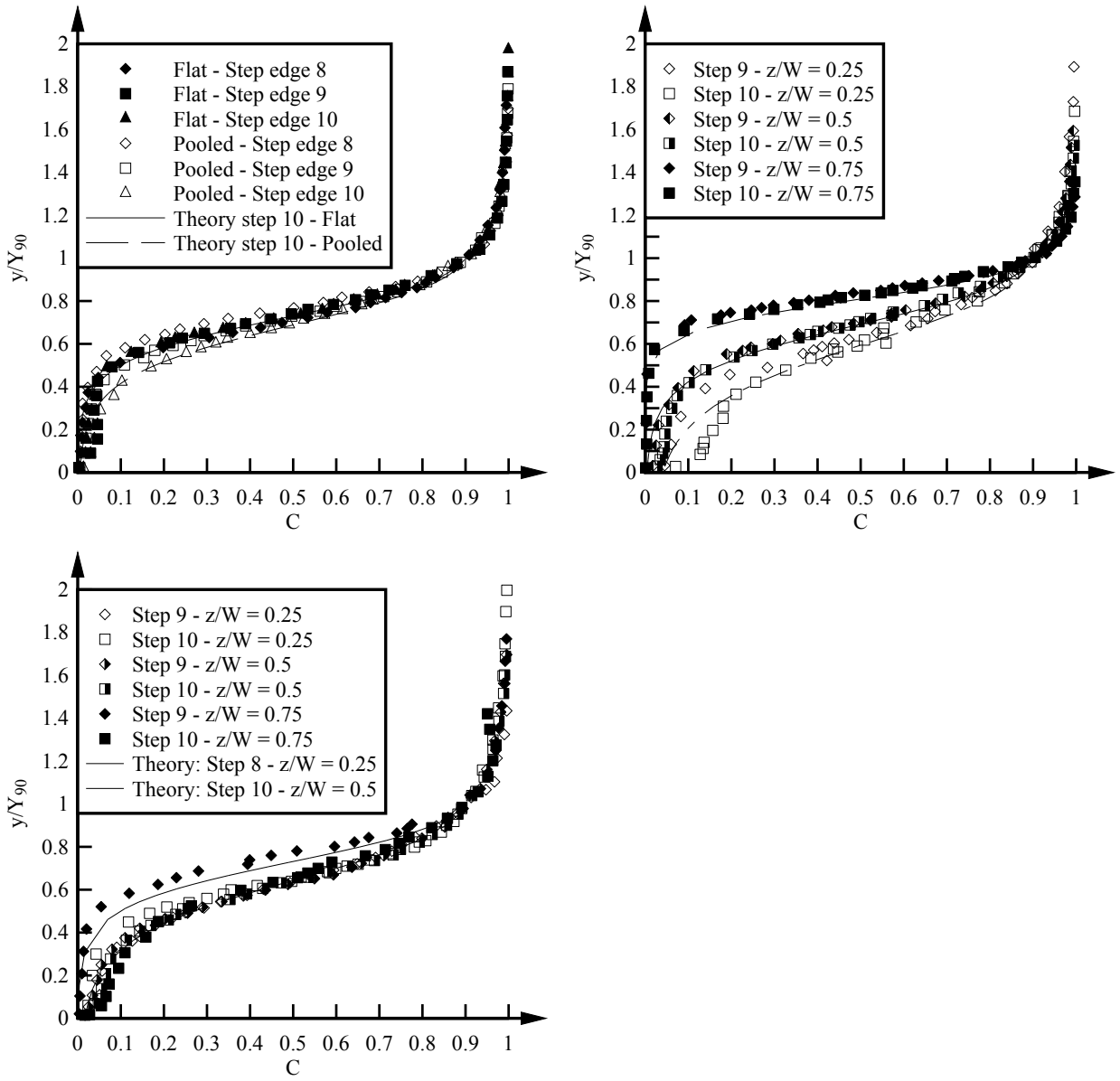

Figure 8. Dimensionless distributions of void fractions in skimming flows - Top left: flat and pooled steps, Q = 0.097 m^3/s, d_c/h = 1.52, Re = 7.4×10^5; Top right: in-line configuration, Q = 0.090 m^3/s, d_c/h = 1.45, Re = 6.9×10^5; Bottom: staggered configuration, Q = 0.113 m^3/s, d_c/h = 1.70, Re = 8.7×10^5

$$H_{res} = d\times\cos\theta + \frac{U_w{}^2}{2\times g} + w = \int_0^{Y_{90}} (1-C)\times\cos\theta\times dy + \frac{q^2}{2\times g\times\left(\int_0^{Y_{90}} (1-C)\times dy\right)^2} + w \quad (5)$$

where d = equivalent clear water depth, q = water discharge per unit width, U_w = flow velocity (U_w = q/d) and w = pool height (w = 0 for flat steps). On the in-line and staggered configurations of flat and pooled steps, the residual head was averaged in the transverse direction (Felder et al. 2012).

For the 10-steps chute, the rate of energy dissipation ranged from 45% to 90%, with decreasing rate of energy dissipation with increasing flow rate as previously observed by Chanson (1994) and Peruginelli and Pagliara (2000). For the design engineers, however, the dimensionless residual head H_{res}/d_c is a more pertinent design parameter. Present results implied that the dimensionless residual head was about $2.5 \leq H_{res}/d_c \leq 5$ (Fig. 9). In Figure 9, the dimensionless residual head is shown as a function of the dimensionless discharge d_c/h. The present data showed the smallest residual head for the flat stepped spillway: i.e., $H_{res}/d_c \approx 3.1$ on average in skimming flow. The residual head was larger on the pooled stepped spillway: i.e., $H_{res}/d_c \approx 3.7$. For the stepped spillways with in-line and staggered configurations of flat and pooled steps, larger residual head data were obtained, with some data scatter.

The data for the in-line and staggered configurations of flat and pooled steps must be considered with care. The results shown in Figure 9 were transverse averaged. Locally the residual head could be signifi-

cantly larger because of the three-dimensional flow motion. For example, on the in-line geometry, the dimensionless residual head H_{res}/d_c ranged from less than 2 to up to 17 locally, depending upon the transverse location and flow rate, while H_{res}/d_c varied within a factor 2 across the last step for a given flow rate on the staggered geometry.

Overall the present data ($\theta = 26.6°$) showed a larger rate of energy dissipation on the spillway with flat horizontal steps compared to all the other configurations in the skimming flow regime. The result was consistent with physical data down a 30° stepped chute (Kökpinar 2004), despite some quantitative difference in residual head levels with the present data (Fig. 9). The finding is contrary to observations on smaller slopes on which the largest rate of energy dissipation was observed with the pooled stepped design (Thorwarth 2008). Herein the designs with in-line and staggered configurations of flat and pooled steps did not provide any advantageous performances in terms of energy dissipation, while they were affected by flow instabilities and three-dimensional patterns leading to some flow concentration.

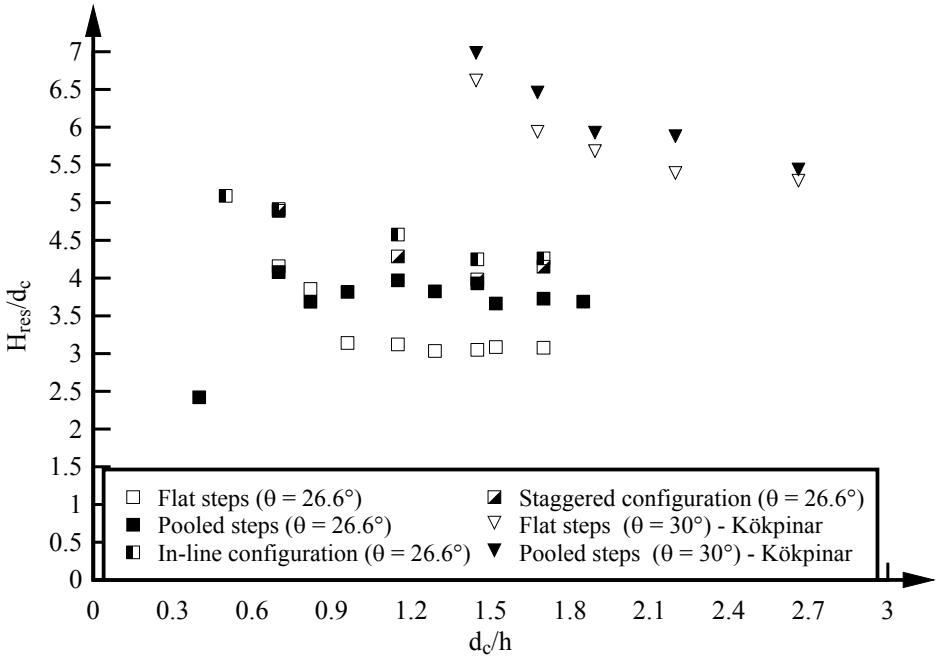

Figure 9. Dimensionless residual head at the downstream end of 10-steps stepped spillways - Comparison between flat stepped chute, pooled step chute, and in-line and staggered configurations of flat and pooled steps (Present study), as well as with the re-analysed data of Kökpinar (2004) - All data were estimated based upon detailed air-water flow measurements

7 CONCLUSION

A physical study was performed on flat and pooled stepped spillways for overflow weirs and embankments ($\theta = 26.6°$). While different stepped chute configurations were tested, the focus of the study was on the cavity flow processes, flow aeration and energy dissipation performances.

The flat stepped spillway showed some typical flow patterns with nappe, transition and skimming flow regimes depending upon the flow rate. Some similar flow regimes were observed on the pooled stepped spillway, although some pulsating flow was seen for some nappe flow rates associated with the downstream propagation of small instabilities. On the in-line and staggered configurations of flat and pooled steps, the flow was highly three-dimensional. Standing sidewall waves and shockwaves were observed along the sidewalls and on channel centreline respectively. These instabilities were instationary and associated with some strong splashing. Detailed air-water flow measurements were conducted downstream of the inception point of free-surface aeration for all configurations. The results highlighted the strong flow aeration. The residual head and energy dissipation rates at the stepped chute downstream end were calculated based upon the air-water flow properties. The results showed that the residual energy was the lowest for the flat stepped weir. The data for the stepped spillway configuration with in-line and staggered configurations of flat and pooled steps showed large differences in terms of residual head in the transverse direction. Altogether the present study demonstrated that, on a 26.6° slope stepped chute, the designs with in-line and staggered configurations of flat and pooled steps did not provide any advantageous performances in terms of energy dissipation and flow aeration, but they were affected by three-dimensional pat-

terns leading to some flow concentration. Another outcome is that some detailed physical investigations for complex stepped spillway designs are strongly recommended before any implementation into a prototype environment.

8 ACKNOWLEDGEMENTS

The authors thank Jason Van Der Gevel and Stewart Matthews (The University of Queensland) for their technical assistance. The financial support of the Australian Research Council (Grant DP120100481) is acknowledged.

REFERENCES

ASCE (1994). Alternatives for Overtopping Protection of Dams. ASCE, New York, USA, Task Committee on Overtopping Protection, 139 pages.

Chamani, M.R. (2000). Air Inception in Skimming Flow Regime over Stepped Spillways. proc. Intl Workshop on Hydraulics of Stepped Spillways, Zürich, Switzerland, Balkema Publ., pp. 61-67.

Chanson, H. (1994). Comparison of Energy Dissipation between Nappe and Skimming Flow Regimes on Stepped Chutes. Journal of Hydraulic Research, IAHR, Vol. 32, No. 2, pp. 213-218. Errata: Vol. 33, No. 1, p. 113.

Chanson, H. (1995). Hydraulic Design of Stepped Cascades, Channels, Weirs and Spillways. Pergamon, Oxford, UK, Jan., 292 pages.

Chanson, H. (2001). The Hydraulics of Stepped Chutes and Spillways. Balkema, Lisse, The Netherlands, 384 pages.

Chanson, H. (2009a). Embankment Overtopping Protections System and Earth Dam Spillways. in Dams: Impact, Stability and Design, Nova Science Publishers, Hauppauge NY, USA, Ed. W.P. HAYES and M.C. BARNES, Chapter 4, pp. 101-132.

Chanson, H. (2009). Turbulent Air-water Flows in Hydraulic Structures: Dynamic Similarity and Scale Effects. Environmental Fluid Mechanics, Vol. 9, No. 2, pp. 125-142 (DOI: 10.1007/s10652-008-9078-3).

Chanson, H., and Gonzalez, C.A. (2005). Physical Modelling and Scale Effects of Air-Water Flows on Stepped Spillways. Journal of Zhejiang University SCIENCE, Vol. 6A, No. 3, March, pp. 243-250.

Chanson, H., and Toombes, L. (2002). Air-Water Flows down Stepped chutes: Turbulence and Flow Structure Observations. Intl Jl of Multiphase Flow, Vol. 27, No. 11, pp. 1737-1761.

Chanson, H., Yasuda, Y., and Ohtsu, I. (2002). Flow Resistance in Skimming Flows and its Modelling. Can. Jl of Civil Engineering, Vol. 29, No. 6, pp. 809-819.

Djenidi, L., Elavarasan, R. and Antonia, R.A. (1999). The Turbulent Boundary Layer over Transverse Square Cavities. Jl of Fluid Mechanics, Vol. 395, pp. 271-294.

Felder, S., and Chanson, H. (2009). Turbulence, Dynamic Similarity and Scale Effects in High-Velocity Free-Surface Flows above a Stepped Chute. Experiments in Fluids, Vol. 47, No. 1, pp. 1-18 (DOI: 10.1007/s00348-009-0628-3).

Felder, S., and Chanson, H. (2012). Air-Water Flow Measurements in Instationary Free-Surface Flows: a Triple Decomposition Technique. Hydraulic Model Report No. CH85/12, School of Civil Engineering, The University of Queensland, Brisbane, Australia, 161 pages.

Felder, S., Guenther, P., and Chanson, H. (2012). Air-Water Flow Properties and Energy Dissipation on Stepped Spillways: a Physical Study of Several Pooled Stepped Configurations. Hydraulic Model Report No. CH87/12, School of Civil Engineering, The University of Queensland, Brisbane, Australia, 225 pages.

Gonzalez, C.A., and Chanson, H. (2008). Turbulence and Cavity Recirculation in Air-Water Skimming Flows on a Stepped Spillway. Jl of Hydraulic Research, IAHR, Vol. 46, No. 1, pp. 65-72.

Kökpinar, M.A. (2004). Flow over a Stepped Chute with and without Macro-Roughness Elements. Can. Jl of Civil Eng., Vol.. 31, No. 5, pp. 880-891.

Ohtsu, I., Yasuda, Y., and Takahashi, M. (2004). Flow Characteristics of Skimming Flows in Stepped Channels. Jl of Hyd. Engrg., ASCE, Vol. 130, No. 9, pp. 860-869.

Peruginelli, A., and Pagliara, S. (2000). Energy Dissipation Comparison among Stepped Channel, Drop and Ramp Structures. Proc. Intl Workshop on Hydraulics of Stepped Spillways, Zürich, Switzerland, Balkema Publ., pp. 111-118.

Peyras, L., Royet, P., and Degoutte, G. (1992). Flow and Energy Dissipation over Stepped Gabion Weirs. Jl of Hyd. Engrg., ASCE, Vol. 118, No. 5, pp. 707-717.

Pfister, M., and Chanson, H. (2012). Scale Effects in Physical Hydraulic Engineering Models. Journal of Hydraulic Research, IAHR, Vol. 50, No. 2, pp. 244-246.

Rajaratnam, N. (1990). Skimming Flow in Stepped Spillways. Jl of Hyd. Engrg., ASCE, Vol. 116, No. 4, pp. 587-591.

Takahashi, M., Yasuda, Y., and Ohtsu, I. (2008). Flow Patterns and Energy Dissipation over Various Stepped Chutes. Discussion. Jl of Irrigation and Drainage Engineering, ASCE, Vol. 134, No. 1, pp. 114-116.

Thorwarth, J. (2008). Hydraulisches Verhalten der Treppengerinne mit eingetieften Stufen – Selbstinduzierte Abflussinstationaritäten und Energiedissipation. (Hydraulics of Pooled Stepped Spillways – Self-induced Unsteady Flow and Energy Dissipation.) Ph.D. thesis, University of Aachen, Germany (in German).

Toombes, L., and Chanson, H. (2007). Surface Waves and Roughness in Self-Aerated Supercritical Flow. Environmental Fluid Mechanics, Vol. 7, No. 3, pp. 259-270 (DOI 10.1007/s10652-007-9022-y).

Wood, I.R. (1991). Air Entrainment in Free-Surface Flows. IAHR Hydraulic Structures Design Manual No. 4, Hydraulic Design Considerations, Balkema Publ., Rotterdam, The Netherlands, 149 pages.